IOP Publishing Journal of Physics: Conference Series **59** (2007) 413–417
doi:10.1088/1742-6596/59/1/088 Eighth International Conference on Laser Ablation

Computational study of cooling rates and recrystallization kinetics in short pulse laser quenching of metal targets

William H. Duff and Leonid V. Zhigilei*

University of Virginia, Department of Materials Science and Engineering
116 Engineer's Way, Charlottesville, VA 22904-4745

* E-mail: lz2n@virginia.edu

Abstract. Short pulse laser melting and resolidification of a metal target are investigated in continuum and atomistic computer simulations. The cooling rates achievable in laser quenching are calculated within the framework of two-temperature model for a range of laser fluences and pulse durations. A well-defined maximum in the cooling rate dependence on the pulse duration and fluence is observed and explained by the competition between the electronic heat conduction and the energy transfer from the electrons to the lattice due to the electron-phonon coupling. The results of molecular dynamics simulations demonstrate that the short pulse laser melting and recrystallization take place under highly non-equilibrium conditions that have a strong effect on the time-scales, rates, and other parameters of all the involved processes. An emission of partial dislocations from the melting front and their retreat at later times is observed in the simulations.

1. Introduction

Short pulse laser processing of metal surfaces typically involves fast transient melting of a thin surface region followed by cooling due to the heat conduction to the bulk of the target and resolidification. The shallow melt depths, typically produced by the short pulse laser irradiation, and the high thermal conductivity of metals can result in very high cooling rates of 10^{12} K/s and more, strong undercooling and rapid resolidification. In particular, high-resolution pump-probe measurements performed for a single crystal Zn target irradiated by a 1 ps laser pulse have yielded times of re-crystallization as short as 100-300 ps [1]. Earlier observations for Si and metallic alloys suggested the lifetime of the melt to be on the order of 1 ns for a 30 ps laser pulse [2,3]. Under the conditions of rapid cooling, the resolidification mechanisms can involve a range of competing processes, including epitaxial regrowth of the substrate, nucleation of crystallites throughout the undercooled melted region, material reheating due to the release of the latent heat of solidification, or formation of an amorphous surface structure. Although significant theoretical and computational efforts have been directed at the analysis of laser melting and resolidification, e.g. [4,5], the understanding of the relationship between the irradiation conditions, cooling rates, and the kinetics of resolidification is still incomplete.

In this paper we report the results of a computational investigation of the cooling rates and recrystallization kinetics in short pulse laser quenching of metal targets. The cooling rates achievable in short pulse laser quenching are first estimated with a conventional two-temperature model (TTM). The kinetics and mechanisms of melting and resolidification of a surface layer occurring under conditions of strong overheating and undercooling are then investigated in a series of molecular dynamics (MD) simulations.

2. TTM calculation of cooling rates in laser quenching

In this section we present the results of TTM calculations of the cooling rates achievable in laser quenching, performed for a range of laser fluences and pulse durations. In TTM model [6], commonly used in the analysis of short-pulse laser interactions with metals, the time evolution of the lattice and electron temperatures, T_l and T_e, is described by two coupled non-linear differential equations,

$$C_e(T_e)\frac{\partial T_e}{\partial t} = \nabla(K_e(T_e)\nabla T_e) - G(T_e - T_l) + S(z,t) \quad (1)$$

$$C_l(T_l)\frac{\partial T_l}{\partial t} = \nabla(K_l(T_l)\nabla T_l) + G(T_e - T_l) \quad (2)$$

where C and K are the heat capacities and thermal conductivities of the electrons and lattice as denoted by subscripts e and l, and G is the electron-phonon coupling constant. The source term S(z,t) is used to describe the local laser energy deposition per unit area and unit time during the laser pulse duration.

The calculations are performed for Ni targets with the following material parameters [7]: $C_e = \gamma T_e$ with γ = 1065 $Jm^{-3}K^{-2}$, $K_e = K_0 T_e/T_l$ with K_0 = 91 $Wm^{-1}K^{-1}$, G = 3.6×10^{17} $Wm^{-3}K^{-1}$. The temperature dependence of the lattice heat capacity is described by the following empirical equations [8]: C_l=4.26+0.0064×T_l $CalK^{-1}mol^{-1}$ for T_l from 293 K to 626 K, C_l=6.99+0.000905×T_l $CalK^{-1}mol^{-1}$ for T_l from 626 K to 1728 K, and a constant heat capacity of 8.55 $CalK^{-1}mol^{-1}$ for the liquid phase. The source term has a Gaussian temporal profile and the optical penetration depth of 13.5 nm is used in the calculations. The laser spot size is assumed to be much larger than the depth affected by the laser heating, allowing us to use a one dimensional version of the model. The system of equations (1) and (2) is solved by a finite difference method and the spatial and time evolution of the electron and lattice temperatures are obtained. The size of the computational domain is chosen so that no significant temperature increase is observed at the back end of the system. The melting process is included into TTM calculation by a simple assumption that as soon as the melting temperature is reached in a given cell of the finite difference discretization, all the additional energy supplied to the lattice by the heat conduction and transferred from the hot electrons through the electron–phonon coupling goes to the latent heat of melting until all the material in the cell is melted.

An example of TTM calculation of the evolution of the surface temperature in a bulk Ni target irradiated by a short laser pulse is shown in Figure 1. The initial lattices heating due to the energy transfer from the hot electrons takes about 20 ps and turns into cooling due to the fast electron heat conduction to the bulk of the target at later times. A surface region melts as the lattice temperature exceeds the equilibrium melting temperature and resolidifies upon cooling. The resolidification process is reflected in a constant temperature plateau in the lattice temperature profile. The resolidification of the top 1 nm surface layer starts at t_1=63 ps and ends at t_2=141 ps. The time of resolidification can be used to estimate the energy flux from the surface layer which, in turn, can be translated to the cooling rate using an average of the values of heat capacities of the solid and liquid phases at the melting temperature. The results of the

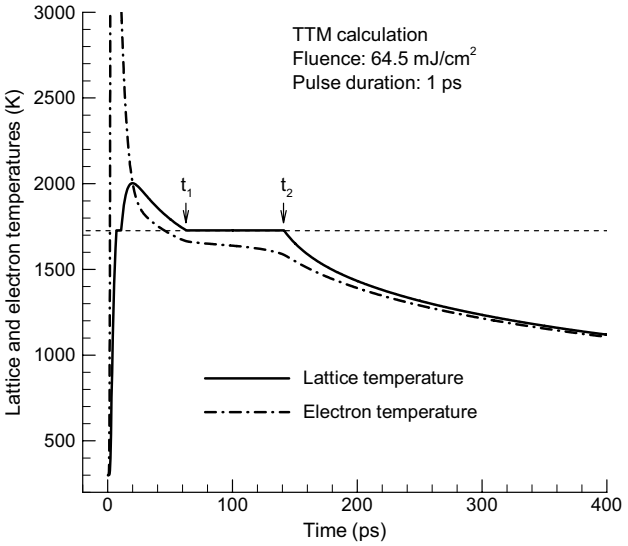

Figure 1. Time dependence of the electron and lattice temperatures of the top 1 nm surface layer of a bulk Ni target irradiated with a 1 ps laser pulse at an absorbed fluence of 64.5 mJ/cm^2, as predicted in a TTM calculation. The horizontal dashed line shows the equilibrium melting temperature of Ni.

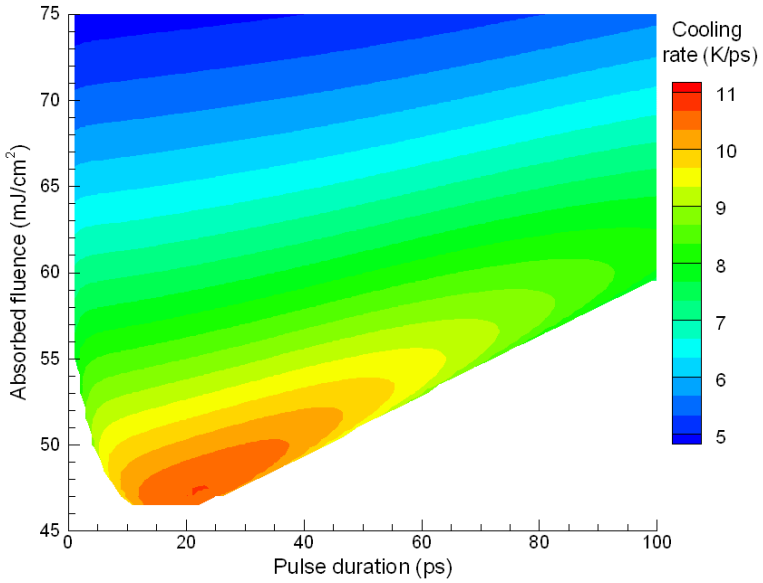

Figure 2. Cooling rates at the time of resolidification calculated with TTM for the top 1 nm layer of a Ni target irradiated by a shot laser pulse. The cooling rates are calculated from the time of resolidification using the values of the latent heat of melting and heat capacities of the solid and liquid phases at the melting temperature. The obtained values of cooling rates are in between the ones of the liquid phase just before the beginning of the resolidification process and the solid phase just after the complete resolidification.

calculation of the surface cooling rates at the time of resolidification are presented in Figure 2. The calculations are performed for pulse duration from 1 to 100 ps in increments of 1 ps and for absorbed fluences from 45 to 75 mJ/cm^2 in increments of 0.5 mJ/cm^2. Only points where the complete melting of the top 1 nm layer of the target occurs are plotted.

In general, the cooling rates predicted by TTM calculations increase with decreasing laser fluence and, for a fixed fluence, with increasing pulse duration. At low fluences, a well-defined maximum of about 10^{13} K/s is observed in the contour plot at pulse durations around 23 ps and absorbed fluences around 47 mJ/cm^2. The position of the maximum of the cooling rate as well as the absence of complete melting at the same laser fluence but shorter laser pulses can be explained by the competition between the electronic heat conduction and the energy transfer from the electrons to the lattice. The thermal conductivity of the electrons depends linearly on the electron temperature and, for laser pulses shorter than the time of electron-phonon equilibration, the initial energy transfer from the surface is faster and the energy transferred to the lattice is not sufficient for the complete melting of the surface layer. Note that the results presented in Figures 1 and 2 are obtained with a very simple model that does not allow for lattice overheating/undercooling and does not include a realistic description of the kinetics of the melting/resolidification process. The results of MD simulations of melting and resolidification, briefly discussed in the next section, demonstrate that both the cooling rates and the characteristic time-scales of the melting and resolidification processes are strongly affected by non-equilibrium conditions created in the target material by short pulse laser irradiation.

3. MD simulations of melting and resolidification

A small depth of the melted layer and a short time of the melting-solidification cycle make this phenomenon amendable to large-scale MD simulations. In this section we briefly discuss the results of a series of simulations performed with a model combining the classical MD method for simulation of nonequilibrium processes of lattice superheating and fast phase transformations with a continuum TTM description of the laser excitation and subsequent relaxation of the conduction band electrons [9]. The parameters of the model are similar to the ones used in simulations of laser interaction with bulk targets in Refs. [10,11] and will be described in more details in a forthcoming paper.

The evolution of the melting and resolidification process is illustrated in Figure 3, where the amount of melted material is shown as a function of time for simulations performed at four different fluences. At low fluencies (43 and 64.5 mJ/cm^2 in Figure 3) we observe a fast homogeneous melting of a surface region, immediately followed by epitaxial recrystallization. At higher fluences (107.5 and

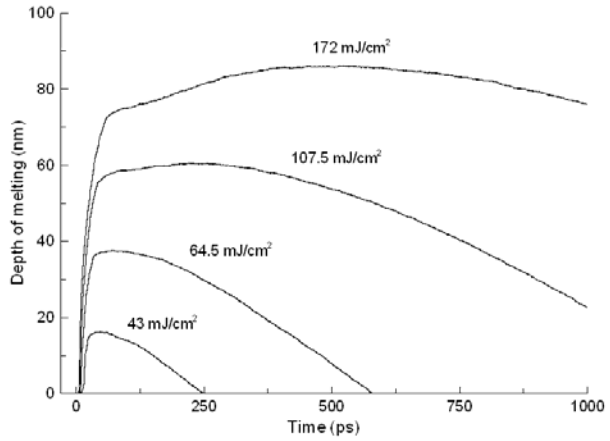

Figure 3. Evolution of the melting depth observed in TTM-MD simulations performed at laser fluences of 43, 64.5, 107.5, and 172 mJ/cm^2 and a pulse duration of 1 ps.

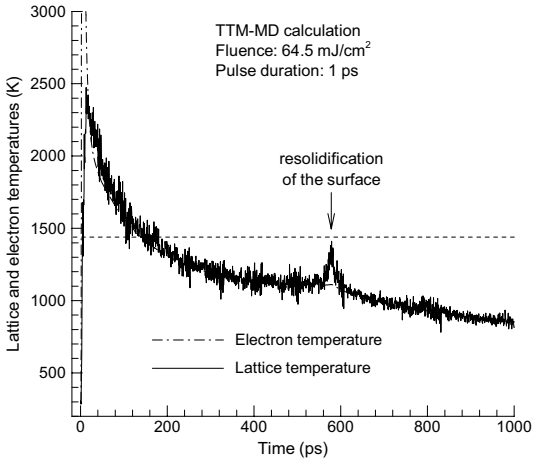

Figure 4. Time dependence of T_e and T_l of the top 1 nm surface layer in a TTM-MD simulation. The dashed line shows the equilibrium melting temperature of the model Ni material [9].

172 mJ/cm^2 in Figure 3) the melting process has two components, a fast homogeneous melting of a large surface layer followed by a slower heterogeneous melting that proceed by the advancement of the liquid-crystal interface formed by the end of the homogeneous melting process.

The resolidification takes place under conditions of strong undercooling below the equilibrium melting temperature, as can be seen from Figure 4, where the evolution of surface temperature is shown for a simulation performed at the same laser fluence of 64.5 mJ/m^2 as the TTM calculation illustrated in Figure 1. The time when the recrystallization front reaches the surface of the target can be identified by a temperature spike associated with the release of the latent heat of melting upon crystallization. There are significant differences between the predictions of the TTM calculation, where crystallization of the surface takes place at the equilibrium melting temperature (Figure 1), and the results of the TTM-MD simulation, where crystallization takes place under conditions of about 23% undercooling below the equilibrium melting temperature at a much later time of about 580 ps (Figure 4). The difference in the time of recrystallization also results in a large difference in the cooling rates. At the time of surface recrystallization the cooling rate is estimated to be about 9×10^{11} K/s in the TTM-MD simulation and about 6×10^{12} K/s in the TTM calculation. At the same time, the cooling rate measured in the TTM-MD simulation at the time when the temperature of the surface reaches the equilibrium melting temperature of the model Ni material (1439 K [9]) compares more favorably with the prediction of the TTM model. We can conclude that simple TTM calculations are not appropriate for quantitative analysis of the phase transformations induced by short pulse laser irradiation and can only be used for rough qualitative estimations.

A detailed analysis of the structure of liquid-crystal interface that develops by the end of the homogeneous stage of the melting process reveals an effect of the emission of partial dislocations that leave behind stacking faults in the original FCC structure, Figure 5. The dislocations are partially retreating back to the interface during the recrystallization process. The emission of the dislocations contributes to the roughening of the melting front and is discussed in details in a forthcoming paper.

4. Summary

Short pulse laser melting and resolidification of a metal target are investigated with TTM and in atomistic computer simulations. The cooling rates achievable in laser quenching are first calculated with TTM for a broad range of laser fluences and pulse durations. A well-defined maximum in the cooling rate dependence on the laser pulse duration and fluence is observed close to the melting

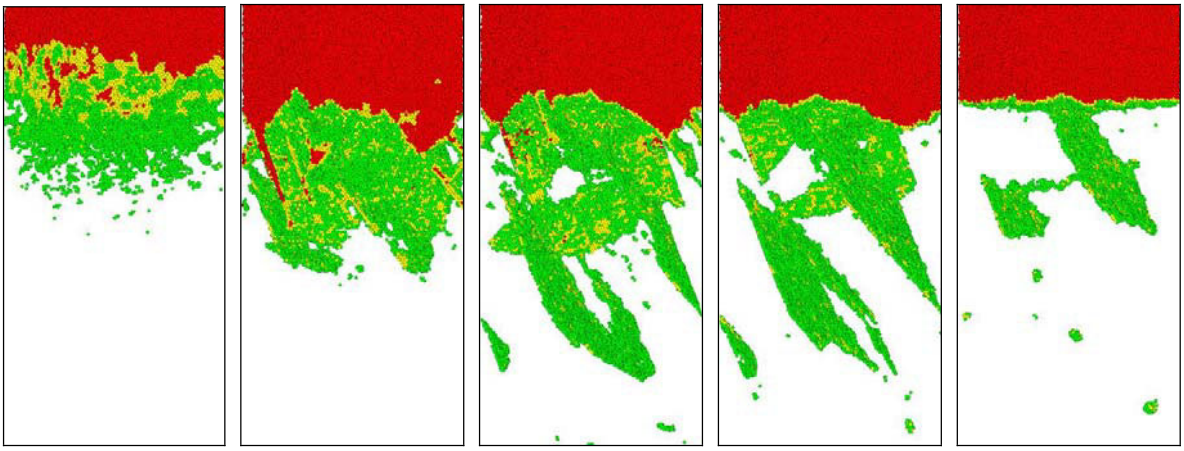

Figure 5. Melting and reversible plastic deformation at of a bulk Ni target observed in a TTM-MD simulation performed at an absorbed fluence of 193.5 mJ/cm^2 and a pulse duration of 1 ps. Atoms are colored according to the local order parameter [9] - red atoms belong to the liquid phase, green atoms correspond to regions of partial local ordering at the interface between the liquid and crystal phases as well as along the planes of the stacking faults left behind by partial dislocations emitted from the liquid-crystal interface. The atoms that have local crystalline (FCC) surroundings are not shown in the snapshots.

threshold at pulse durations around 23 ps. The maximum is defined by the competition between the energy transfer from the electrons to the lattice and the temperature-dependent electronic heat conduction to the bulk of the target. The results of molecular dynamics simulations demonstrate that the short pulse laser melting and recrystallization take place under highly non-equilibrium conditions that have a strong effect on time-scales, rates, and other parameters of all the involved processes. Simple TTM calculations are not appropriate for quantitative analysis of phase transformations induced by short pulse laser irradiation and can only be used for qualitative estimations.

Acknowledgments

Financial support of this work is provided by the NSF through award CTS-0348503 and by the ONR through a sub-contract from the Electro-Optics Center, Penn State University.

References

[1] Agranat M B, Ashitkov S I, Fortov V E, Kirillin A V, Kostanovskii A V, Anisimov S I and Kondratenko P S 1999 *Appl. Phys. A* **69**, 637-40

[2] Lin C-J, Spaepen F and Turnbull D 1984 *J. Non-Cryst. Solids* **61-62**, 767-72

[3] MacDonald C A, Malvezzi A M and Spaepen F 1989 *J. Appl. Phys.* **65**, 129-36

[4] Kapat J S, Wei Z and Kumar A 1998 Appl. Surf. Sci. **127-129**, 212-7

[5] Xu X, Chen G and Song K H 1999 *Int. J. Heat Mass Transfer* A **42**, 1371-82

[6] Anisimov S I, Kapeliovich B L and Perel'man T L 1974 *Sov. Phys. JETP* **39**, 375-7

[7] Hohlfeld J, Wellershoff S-S, Güdde J, Conrad U, Jähnke V and Matthias E 2000 *Chem. Phys.* **251**, 237-58

[8] Perry's Chemical Engineers' Handbook, 7th edition 1997, ed R H Perry, D W Green and J O Maloney (New York: McGraw-Hill) p 2-165

[9] Ivanov D S and L V Zhigilei 2003 *Phys. Rev. B* **68**, 064114

[10] Leveugle E, Ivanov D S and Zhigilei L V 2004 *Appl. Phys. A* **79**, 1643-55

[11] Zhigilei L V, Ivanov D S, Leveugle E, Sadigh B and Bringa E M 2004 *Proc. SPIE* **5448** 505-19